FRACTURE OF CSL BOUNDARIES IN CU AND AL

Douglas E. Spearot,[1] Karl I. Jacob[2] and David L. McDowell[1,3]

[1]G.W. Woodruff School of Mechanical Engineering, Georgia Institute of Technology, Atlanta GA, 30332 USA
[2]School of Polymer, Textile & Fiber Engineering, Georgia Institute of Technology, Atlanta GA, 30332 USA
[3]School of Materials Science and Engineering, Georgia Institute of Technology, Atlanta GA, 30332 USA

ABSTRACT

Molecular dynamics (MD) simulations using embedded-atom method (EAM) potentials are used to study the fundamental failure processes that occur on the nanoscale in copper and aluminum as a result of an applied boundary deformation. This work focuses on tensile deformation and fracture of 'near' and 'exact' Coincident Site Lattice (CSL) grain boundaries. Previous experimental and simulation work has shown that grain boundaries with CSL misorientations may have a lower grain boundary energy, which suggests that these boundaries may have unique fracture properties as compared with general high-angle grain boundaries. In this communication we study grain boundary interface models formed by a symmetric rotation of the opposing lattice regions around a [100] misorientation axis. Interface structures are created using a 0 K energy minimization procedure with a nonlinear conjugate gradient algorithm. Tensile deformation calculations are performed at 300 K using appropriate temperature controls. For the range of interface misorientation angles examined in this work, the interface structure appears to play a role in the tensile deformation response. Specifically, the peak tensile stress within the interface region shows a modest increase for interface models with exact $\Sigma5$ (310) orientation in copper and exact $\Sigma5$ (210) orientation in aluminum. Interface models with near $\Sigma5$ interface misorientations show a reduced peak stress by comparison. An approximation of interface porosity on the nanoscale is calculated by monitoring the coordination number of each atom within the interface region. MD simulations show that the nanoporosity measurement is capable of differentiating between grain boundaries on the nanoscale, and thus is appropriate to relate the interface structure to the interface strength for the purpose of making connections to microstructure-sensitive continuum interface separation potentials.

1 INTRODUCTION

It has been documented that the atomic structure of grain boundary interfaces has an effect on certain properties of crystalline materials [1,2]. This phenomenon is magnified in nanocrystalline structures as a greater percentage of atoms are situated in close proximity to grain boundary interfaces. Grain boundaries may be described using a misorientation angle/axis notation. Grain boundaries for which the normal to the grain boundary plane is perpendicular to the grain boundary misorientation axis are defined as 'tilt' interfaces. Although tilt grain boundaries compose a very small portion of the total set of grain boundary angle/axis combinations, they have been observed experimentally, suggesting that they may be energetically favorable as compared with general high-angle grain boundaries [3]. A smaller subset of tilt interfaces are considered 'geometrically special' in the sense that the opposing lattice regions will 'fit' more closely along the grain boundary interface plane [1,2]. These special grain boundaries are characterized by the density of coincident atomic sites between the opposing lattice regions. For a specific angle/axis combination, two interpenetrating lattices will mathematically create a three-dimensional array of coincident lattice points in which 1 in Σ sites are coincident. The Σ coincident site lattice (CSL) model notation is used to describe specific angle/axis combinations in this work.

The goal of this research work is to investigate the relationship between nanoscale grain boundary structure and interface decohesion properties. We ultimately aim to make a

connection to the continuum interface separation methodology of Needleman [4]. In Needleman's work, the traction on a crack surface is related to the displacement jump across that crack surface through an interface separation potential. Three parameters are important in the description of the interface potential: the peak interface strength, the displacement associated with the peak interface strength and the work of separation for the interface. In this communication we perform atomistic calculations of tensile interface separation on a small subset of symmetric tilt grain boundaries to identify trends or relationships between the tensile interface properties and the grain boundary misorientation angle. Results show that certain CSL grain boundaries have increased grain boundary interface strength relative to general grain boundary interface misorientations, but the effect is not pronounced.

2 COMPUTATIONAL PROCEDURE

To model the interatomic interactions, the embedded-atom method (EAM) potentials of Mishin *et al*. for copper [5] and aluminum [6] are used in this work. The EAM potentials of Mishin *et al.* are fit to a host of material properties from both experiment and *ab initio* calculations, including the lattice constant, the cohesive energy, elastic constants and various surface and defect energies. Calculations in Zimmerman *et al*. [7] confirm that the Mishin *et al*. potential for aluminum accurately predicts the <112> stable stacking fault energy. Independent calculations by the current authors have confirmed that the Mishin *et al.* EAM potential for copper also correctly reproduces the stacking fault energy.

In this communication, we consider grain boundary interface models formed by symmetric lattice rotations around a [001] grain boundary misorientation axis. Periodic boundary conditions are applied to the model boundaries that are perpendicular to the grain boundary interface plane. The dimensions of the interface model in these directions are defined as necessary to properly enforce periodicity. Nonperiodic boundary conditions are used on the boundaries that are parallel to the grain boundary interface plane. Constraints are placed on atoms that lie along these boundaries to stipulate that these surfaces remain planar and parallel during the energy minimization, thermal equilibration and tensile deformation processes. The height of the grain boundary interface model are taken as $H = 12\lambda$; where λ is the lattice constant of either copper (3.615 Å) or aluminum (4.050 Å). Depending on the dimensions in the periodic directions, the grain boundary interface models contain between 20,000 and 35,000 atoms.

Energy minimization calculations at 0 K are performed to construct the grain boundary interface models considered in this work. A nonlinear conjugate gradient algorithm is used to calculate the atomic positions associated with the minimum potential energy of the interface
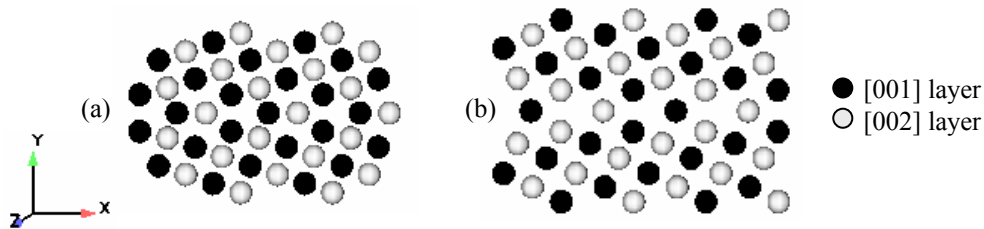

Figure 1. (a) Σ5 (310) 36.9° grain boundary interface structure after 0 K energy minimization; (b) Σ5 (210) 53.1° grain boundary interface structure after 0 K energy minimization.

(most probable configuration). During the energy minimization process, the boundaries of the interface model parallel to the grain boundary plane are allowed to move both perpendicular and parallel to the interface. It is critical to allow for relative translations of the opposing lattice regions to construct realistic grain boundary interface models [8]. When searching for the minimum energy configuration, a number of initial starting positions are used to ensure that the grain boundary structures calculated are not metastable structures, but are truly the minimum energy configurations. Figure 1 shows the grain boundary interface structure for (a) $\Sigma 5$ (310) 36.9^o grain boundary interface in copper and (b) $\Sigma 5$ (210) 53.1^o grain boundary interface in aluminum after the 0 K energy minimization. The energies calculated in this work for copper and aluminum $\Sigma 5$ (310) 36.9^o and $\Sigma 5$ (210) 53.1^o grain boundaries match the energies reported by Mishin and coworkers [5,6].

Once the minimum energy configuration is attained through the procedure described above, the grain boundary interface model is dynamically equilibrated to 300 K using a Nose-Hoover constant temperature algorithm [9]. As in the energy minimization procedure, the boundaries of the grain boundary interface model parallel to the grain boundary plane are allowed to move perpendicular and parallel to the interface. Note that the interface structure is preserved during the thermal equilibration procedure.

3 MOLECULAR DYNAMICS RESULTS

The influence of grain boundary interface structure on the fracture response may be determined through a series of molecular dynamics fracture simulations involving normal and shear separation, as well as sequences of normal-shear and shear-normal deformation relative to the interface. In addition, the unloading response of the interface, which is important in characterizing the irreversibility of the interface separation potential [10], may be studied by removing the applied deformation after specific magnitudes of normal and/or tangential deformation.

To deform the interface model in this work, uniform displacement rate boundary conditions are applied to the nonperiodic boundaries of the interface model. The displacement rate boundary condition is uniformly applied over the entire boundary plane. As a result of the constraints placed on these atoms, under application of a prescribed velocity condition each boundary will move as a total unit, remaining planar and parallel during the entire deformation process. The magnitude of the boundary velocity is chosen such that the tensile strain rate for both copper and aluminum interface models is 1.0×10^{10} s^{-1}. This strain rate is extremely high to accommodate the use of a small time step, which is inherent to performing molecular dynamics calculations. Gall *et al*. [11] show that for atomistic interface model scales (most notably the height, H) on the order of those that we have studied in this work, the effect of the elastic stress wave produced by the dynamic strain rate on the deformation response is minimal.

The tensile stress within the interface region is plotted against the interface displacement to analyze the deformation response of each grain boundary interface model. This convention is chosen to maintain an analogy to the traction-displacement form of continuum interface separation potentials [4]. The displacement of the interface region is defined, in this work, as the absolute sum of the displacements of both loading planes. This quantity will be referred to as either 'far-field displacement' or simply as 'displacement'. Atomic stress is calculated using the virial definition averaged over all atoms within the interface region except those in close proximity to the constrained loading boundaries.

Figure 2 shows the tensile separation response for near and exact $\Sigma 5$ (310) 36.9^o grain boundary interface models in copper. Figure 2(a) shows the interface tensile stress-displacement response, while Fig. 2(b) shows the calculation of nanoscale interface porosity
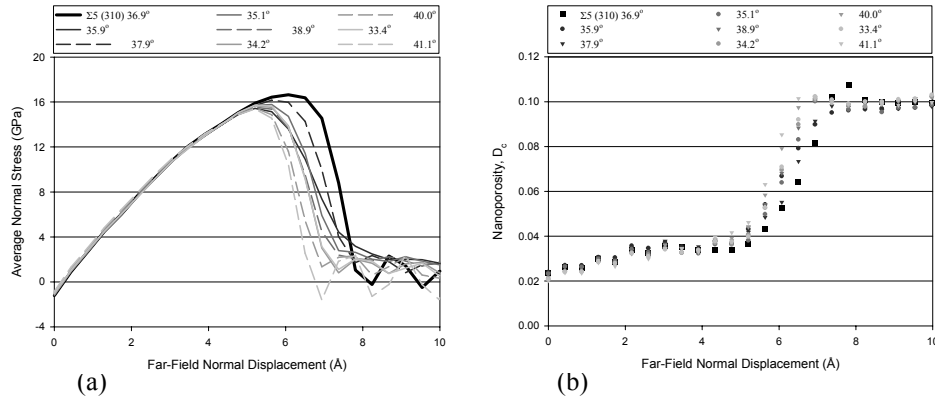
Figure 2: (a) tensile stress versus far-field normal displacement for near and exact Σ5 (310) grain boundaries in copper; (b) Nanoporosity measurement versus far-field normal displacement for near and exact Σ5 (310) copper grain boundaries.

based on the atomic coordination number of each atom within the interface region [10]. The CSL misorientation is shown in black, while the near-CSL grain boundary models are grouped by their proximity to the CSL orientation. In general, the tensile stress within the interface region increases to a peak during tensile extension then decreases to zero signifying complete separation. Dislocations are emitted from the grain boundary interface just prior to the peak tensile stress. The drop in tensile stress is a result of the formation and coalescence of voids along the grain boundary plane. Figure 2 shows that the peak stress during separation and the displacement associated with peak stress appear to be affected by the interface misorientation angle in copper. As the interface model deviates from perfect CSL orientation, the interface strength decreases slightly. Figure 2(b) shows that the nanoporosity measure appears to be capable of differentiating between grain boundary interfaces on the nanoscale. As the misorientation angle deviates from perfect CSL orientation, the porosity developed within the interface region during void formation and coalescence increases slightly. This increase in interface porosity may be related to the decrease in interface properties through an appropriately posed constitutive model.

Figures 3(a) and 3(b) show the tensile stress and nanoporosity calculations versus the interface displacement for aluminum near and exact Σ5 (210) 53.1° grain boundary interface models. Again, the CSL misorientation is shown in black, while the near-CSL grain boundary models are grouped by their proximity to the CSL orientation. The tensile stress-displacement response shows a two-stage behavior in aluminum. Initially, the tensile stress within the interface region increases with a given slope until a tensile deformation of approximately 4.0 Å. This point corresponds to the emission of dislocations from the grain boundary interface. The stress within the interface region continues to increase upon further tensile deformation with a different slope until it reaches a peak magnitude. Increased displacement leads to void formation and coalescence at this point, decreasing the tensile stress to zero, signifying complete separation. Figure 3(a) shows that the grain boundary structure appears to have an effect on the tensile decohesion response of the aluminum interfaces. The Σ5 (210) CSL orientation shows a slightly increased tensile strength relative to the near-CSL interface models, although there is more variation in the aluminum calculation than in copper. Figure 3(b) shows
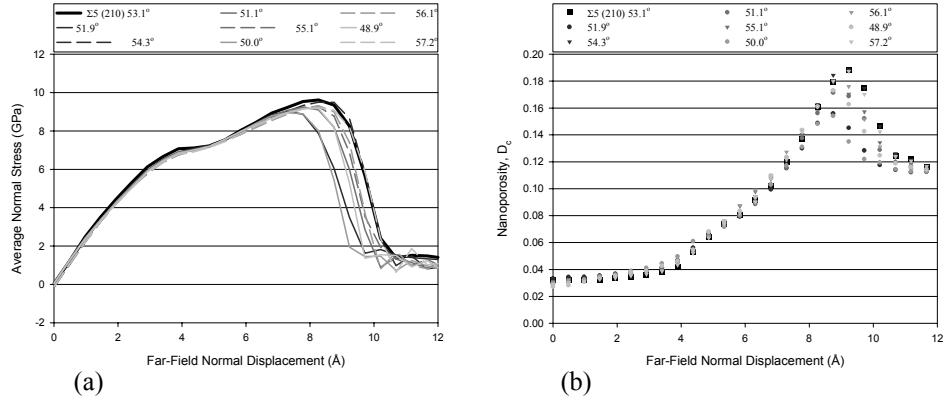
Figure 3: (a) Tensile stress versus far-field normal displacement for near and exact Σ5 (210) grain boundaries in aluminum; (b) Calculation of the nanoporosity measure for near and exact Σ5 grain boundaries in aluminum.

that the nanoporosity measure appears to be capable of differentiating between grain boundaries on the nanoscale in aluminum during the void nucleation and coalescence portion of the stress-displacement curves. Note that at a given interface displacement after the onset of void nucleation, the nanoporosity measure captures the ordering of the grain boundary misorientation models with respect to the interface stress. Further, prior to the point of void nucleation, the nanoporosity measure shows minimal distinction between grain boundary interface models, in agreement with the results shown in Fig. 3(a).

Performing molecular dynamics calculations of tensile separation for a range of grain boundary interface models, the relationship between the peak tensile strength and the grain boundary misorientation angle may be developed. Preliminary results as shown in Figs. 2 and 3 above indicate that the grain boundary structure plays a role in the tensile separation response of each grain boundary interface model.

4 CONCLUSIONS

Atomistic calculations of grain boundary interface separation in copper and aluminum are presented. In this work, we examine grain boundary interface models created by a symmetric rotation of two opposing lattice regions around a [001] grain boundary misorientation axis. Using a nonlinear conjugate gradient algorithm, 0 K energy minimization calculations are performed to determine the structure of each grain boundary interface considered. After an appropriate thermal equilibration procedure, the grain boundary interface models are deformed in tension at 300 K under a constant strain rate to complete separation. Calculations show that for the CSL grain boundary interface models studied in this work, the nanoscale structure of the interface contributes to an increase in the tensile separation properties. For example, the Σ5 (310) CSL lattice model in copper shows an increased tensile strength as compared with near-CSL orientations. Similarly, for aluminum the Σ5 (210) boundary shows an elevated tensile strength. The measurement of nanoporosity within the interface region is capable of differentiating between grain boundary interface misorientations during the void nucleation, growth and coalescence portions of the stress-displacement curves.

Our aim is that these simulations will motivate connections between atomistic calculations of interface decohesion and continuum based interface separation potentials. As shown in Spearot *et al.* [10], the nanoporosity measure may be used as a nanoscale internal state variable when relating the interface structure to the deformation response. It is important to note, however, that the length scale and boundary conditions of these calculations undoubtedly play a role in the tensile deformation response. The calculations performed in this work address interface separation for a small volume of material under a given strain rate and do not consider the influence of the boundary constraints on dislocation emission. As a result of the periodic boundaries, stresses are developed in the nonloading directions (parallel to the interface plane) during the deformation process. Kitamura *et al.* [12] perform a qualitative comparison between free-transverse stress boundary conditions (in a NPT ensemble sense) and fully periodic boundary conditions (NVT ensemble) during deformation of nickel single crystals in tension. They show that stresses developed in the nonloading directions contribute to an increase in the peak tensile strength and a decrease in the ductility of the crystal. Kitamura *et al.* [12] do not extend their study to evaluate if the above conclusion holds for different lattice orientations.

5 ACKNOWLEDGEMENTS

6 REFERENCES

[1]   Howe, J.M., *Interfaces in materials: Atomic structure, thermodynamic and kinetics of solid-vapor, solid-liquid and solid-solid interfaces*, New York, Wiley, 297-371, 1997.

[2]   Randle, V., *The role of the coincidence site lattice in grain boundary engineering*, London, Institute of Materials, 1-128, 1996.

[3]   Sutton, A.P. and Balluffi, R.W., Acta Metallurgica, 35(9), 2177-2201 (1987).

[4]   Needleman, A., Journal of Applied Mechanics, 54(3), 525-531 (1987).

[5]   Mishin, Y., Mehl, M.J., Papaconstantopoulos, D.A., Voter, A.F. and Kress, J.D., Physical Review B, 63(22), 224106-1 (2001).

[6]   Mishin, Y., Farkas, D., Mehl, M.J. and Papaconstantopoulos, D.A., Physical Review B, 59(5), 3393-3407 (1999).

[7]   Zimmerman, J.A., Gao, H. and Abraham, F.F., Modelling and Simulation in Materials Science and Engineering, 8(2), 103-116 (2000).

[8]   Medlin, D.L., Mills, M.J., Stobbs, W.M., Daw, M.S. and Cosandey, F., *HRTEM observations of a Σ=3 {112} bicrystal boundary in aluminum*. in *Symposium on Atomic-scale Imaging of Surfaces and Interfaces,* Materials Research Society, Pittsburgh, PA, USA, 91-96, 1993.

[9]   Hoover, W.G., Physical Review A, 31(3), 1695-1697 (1985).

[10]   Spearot, D.E., Jacob, K.I. and McDowell, D.L., Mechanics of Materials, in press (2003).

[11]   Gall, K., Horstemeyer, M.F., Van Schilfgaarde, M. and Baskes, M.I., Journal of the Mechanics and Physics of Solids, 48(10), 2183-2212 (2000).

[12]   Kitamura, T., Yashiro, K. and Ohtani, R., JSME International Journal A, 40(4), 430-435 (1997).